

# Actif Filter Based Grid Side Converter for Power Quality Enhancement in Wind Turbine Based DFIG

Siham KHELIFA<sup>1</sup>, Abdelhafid SEMMAH<sup>1</sup>

<sup>1</sup>Laboratory of Intelligent Control and Electrical Power System  
Faculty of Science and Technology, University of Djilali Liabès  
Sidi Bel-Abbès, Algeria

E-Mail : siham.khelifa@univ-sba.dz

**Abstract** - The extensive use of power electronics has led to serious power quality issues due to the emission of current harmonics in the utilities. In wind power plants based doubly fed induction generator DFIG, the harmonics can be produced by the converters used to connect the rotor of the DFIG wind turbine to the grid in addition to non linear load connected to it. This paper presents a modeling and control of the grid side converter of wind turbine based doubly -fed induction generator (DFIG) to mitigate the harmonic current from the electrical system and also guarantee the control of the power flow to the grid. A direct voltage vector control is used for the grid side converter. The design methodology of the PI controller is presented. The harmonics were identified using synchronous reference frame SRF. The control methodology is implemented using MATLAB /SIMULINK software and the findings obtained show the performance of this compensation technique in terms of harmonic distortion reduction and power-factor improvement.

**Keywords** -Active filter, wind turbine, power quality, doubly fed induction generator, harmonics, THD.

## I. INTRODUCTION

The integration of wind energy conversions systems in the network to provide electrical energy to consumers has grown especially after the progress that is witnessed in many domains of technology, the growth of population and demand on electrical energy.

The most common wind turbine in the industrial application is equipped with the doubly-fed induction generator DFIG, for the benefits that offers as the independent control of active and reactive power, thus improving power quality and lower converter cost , high and energy yield, variable speed operation (-/+30% around the synchronism speed) [1, 2]. The stator of the doubly-fed induction generator is linked directly to the grid while the rotor of DFIG is connected to the grid throughout power electronic interface called grid side converter GSC and RSC rotor side converter. Each one of them is controlled to achieve a specific function where the control of the grid side converter aims to maintain the dc bus voltage at stable value, and the control of the rotor

side converter has the objective of controlling reactive and active power flow [3, 4].

Harmonics in WT-based DFIG can be produced by GSC and RSC and injected into the grid during rotor speed operation whether in sub-synchronous speed or super-synchronous speed. Harmonics flowing in distribution networks downgrade the quality of electrical power. This can have several negative effects on the operation of all electrical equipment like heating in the transformer connected by way of eddy current losses and skin effect losses. Switch gear relays that are the guards of power system, measurement equipment, and rotating machinery.

The performance of DFIG based WT and its power quality have been proposed and put into practical use and they had proved their capability of ensuring a perfect harmonic compensation, power factor correction, flickers cancellation system equilibration. The APF injects compensating currents to eliminate the harmonic currents from the ac supply. In response to the power quality concerns, typical power distribution networks are requested to obey regulations governing harmonic compliance, in particular IEEE-519 and IEC 61000-3, in terms of

harmonic distortion and power factor [6], the detection and the extraction of harmonics circulating in the ac supply is an important step for a suitable function of the active filter. In the literature, there are two domains of algorithms to identify harmonic references of currents or voltages which are: the frequency domain or the time domain. The methods of identifying harmonics in the time domain are characterized by a fast response time and a minimal computation compared to the methods in the frequency domain [7, 8].

In references [9-11] the active filtering functionality was added to the control algorithm of the GSC in wind power systems with DFIG, the algorithm of detection of harmonic used is instantaneous power theory which is sensitive to unbalanced condition; other studies use a synchronous reference frame which is a simple implementation.

This paper is an exposition of the modeling and simulation of wind turbine based DFIG connected to the grid using vector control for both sides of converters in addition to active filtering in the point of common coupling (PCC) performed by the grid side converter which is connected to the grid in the presence of three-phase full-bridge rectifier feeding a resistive and inductive components.

The control of active and reactive powers of the generator is accomplished through field vector control by stator field. The power control and filtering function occur simultaneously. In harmonic identification, the extraction of the fundamental component is based on the synchronous reference frame SRF theory.

## II. POWER CONTROL OF THE DOUBLY FED INDUCTION GENERATOR – DFIG

In this section, a description of the modeling of DFIG is presented in details. Fig.1 shows a schematic diagram of the studied system that consists of a wind turbine based on a doubly-fed induction generator connected to the grid the stator of the machine is linked directly where the rotor is connected throughout a back to back converter, a nonlinear load is linked to the supply system, at the point of common coupling PCC, an algorithm in time domain based SRF is used to extract harmonics from the system then added to the current generated by dc bus voltage solve the problem of harmonic current

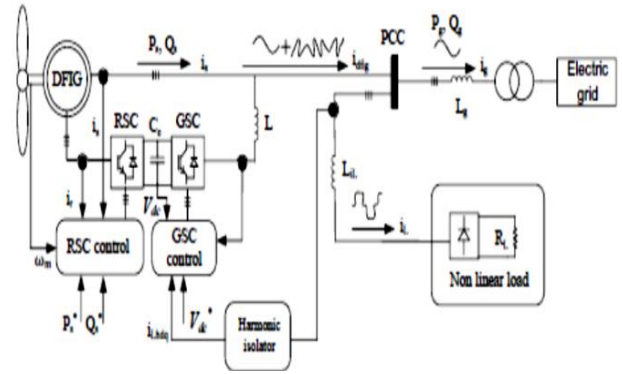


Fig. 1. The principle of harmonic mitigation in wind turbine based DFIG using GSC.

### A) DFIG modeling

The mathematical model of a DFIG in the d-q reference frame is described in the following equation.

$$\begin{cases} V_{ds} = R_s I_{ds} - \omega_s \varphi_{qs} + \frac{d\varphi_{ds}}{dt} \\ V_{qs} = R_s I_{qs} + \omega_s \varphi_{ds} + \frac{d\varphi_{qs}}{dt} \\ V_{dr} = R_r I_{dr} - (\omega_s - \omega_r) \varphi_{qr} + \frac{d\varphi_{dr}}{dt} \\ V_{qr} = R_r I_{qr} + (\omega_s - \omega_r) \varphi_{dr} + \frac{d\varphi_{qr}}{dt} \end{cases} \quad (1)$$

$$\begin{cases} \varphi_{ds} = L_s I_{ds} + L_m I_{dr} \\ \varphi_{qs} = L_s I_{qs} + L_m I_{qr} \\ \varphi_{dr} = L_r I_{dr} + L_m I_{ds} \\ \varphi_{qr} = L_r I_{qr} + L_m I_{qs} \end{cases} \quad (2)$$

$$C_{em} = \frac{3}{2} p \frac{M}{L_s} (\varphi_{qs} I_{dr} - \varphi_{ds} I_{qr}) \quad (3)$$

$$\begin{cases} P_s = \frac{3}{2} (V_{ds} I_{ds} - V_{qs} I_{qs}) \\ Q_s = \frac{3}{2} (V_{qs} I_{ds} - V_{ds} I_{qs}) \end{cases} \quad (a) \quad (4)$$

$$\begin{cases} P_r = \frac{3}{2} (V_{dr} I_{dr} - V_{qr} I_{qr}) \\ Q_r = \frac{3}{2} (V_{qr} I_{dr} - V_{dr} I_{qr}) \end{cases} \quad (b)$$

$V_{ds}$ ,  $V_{qs}$ ,  $V_{dr}$ ,  $V_{qr}$ ,  $\varphi_{dr}$ ,  $\varphi_{qr}$ ,  $\varphi_{ds}$ ,  $\varphi_{qs}$ ,  $C_{em}$ ,  $P_s$ ,  $Q_s$ ,  $P_r$ ,  $Q_r$  denote respectively stator voltage, rotor voltage, rotor flux, stator flux, electromagnetic torque, active and reactive power of stator and the active and reactive power of the rotor.

### B) Control of Rotor-Side Converter

The active and reactive power in the stator can be described by rotor d-axis and q-axis current,

respectively, the vector control and the direct control are most commonly used and representing techniques for both the rotor -side converter and the grid-side converter. The vector control can be further divided into the stator flux-oriented control (FOC) and the stator voltage-oriented control (VOC) by different orientations of the synchronous rotating frame [15, 16]. A flux-oriented control is used for the control of the rotor side converter; the vector of the stator voltage is aligned to the d-axis of the rotating frame for the decoupling control of the active and the reactive power [17]. The control diagram of RSC using FOC is presented in fig. 2

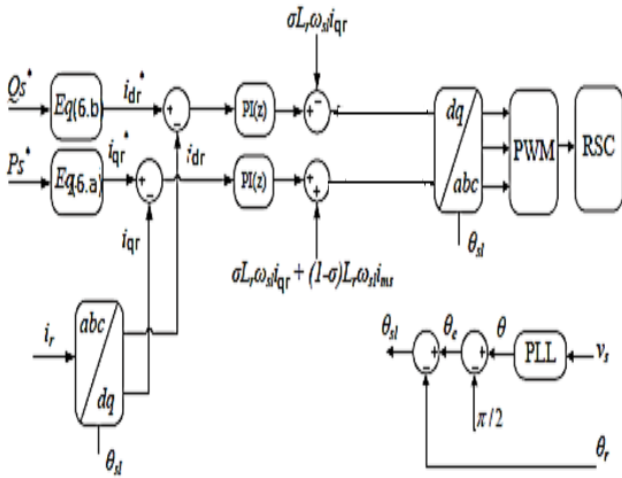


Fig.2. FOC diagram for RSC.

The magnetic flux in the stator in d and q axis is determined by :  $\varphi_{qs}=0$ ;  $d\varphi_{qs}/dt=0$  and  $\varphi_{ds}=\varphi_s$  substituting this condition in the mathematical equation of flux ,currents , active and reactive power of stator the expressions of currents of stator on d axis and q axis are defined by :

$$\begin{cases} I_{qs} = I_{qr} * \frac{-L_m}{L_s} \\ I_{ds} = \frac{\varphi_s}{L_s} - I_{dr} \frac{L_m}{L_s} \end{cases} \quad (5)$$

substituting (5)in (4) the expressions of active and reactive power of stator we obtain :

$$\begin{cases} P_s = -\frac{3}{2} \frac{L_m}{L_s} V_s I_{qr} & (a) \\ Q_s = \frac{3}{2} \frac{L_m}{L_s} V_s (-I_{dr} + \frac{V_s}{L_m \omega_{sr}}) & (b) \end{cases} \quad (6)$$

By substituting (5) in the equations of the flux of the rotor and substituting the expression obtained in the mathematical expressions of the voltage of the rotor, the following expression is obtained :

$$\begin{cases} V_{dr} = R_r I_{dr} + L_r \sigma \frac{dI_{dr}}{dt} - \omega_{sr} L_r \sigma I_{qr} \\ V_{qr} = R_r I_{qr} + L_r \sigma \frac{dI_{qr}}{dt} + \omega_{sr} L_r \sigma I_{dr} + \omega_{sr} \frac{L_m * V_s}{L_s} \end{cases} \quad (7)$$

### C) Control of the grid side converter GSC

The Grid side system is depicted in a d,q axis before the exposure of the vector control-based diagram. This representation provides the mathematical base to understand the grid side system's dynamic action (dynamic model) and then vector control derivation. The system set by the grid side converter, filter, and grid voltage and the following equations can be presented :

$$\begin{cases} V_{df} = R_f I_d + V_d + L_f \frac{dI_d}{dt} - \omega_s L_f I_q \\ V_{qf} = R_f I_q + L_f \frac{dI_q}{dt} + \omega_s L_f \sigma I_d + V_q \end{cases} \quad (8)$$

Where  $L_f$ ,  $R_f$ ,  $V_d$ ,  $V_q$ ,  $V_{df}$ ,  $V_{qf}$  denote respectively inductance filter, resistance filter, grid voltage, grid side converter voltages. The Control of the grid side system is necessary, without it, it is not possible to make the system works properly. In this section a vector control is studied, this technique is widely extended among the control strategies for grid-connected converters. It provides good performance characteristics with reasonably simple implementation requirements, the diagram of the control technique is presented in Fig. 3 and in the proposed active filtering, and an additional current control loop is added as presented in Fig. 4.

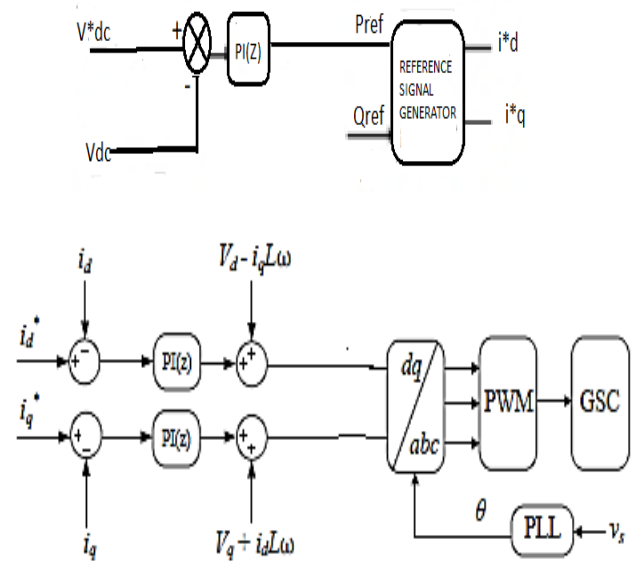


Fig. 3. Control scheme of grid side converter (GSC).

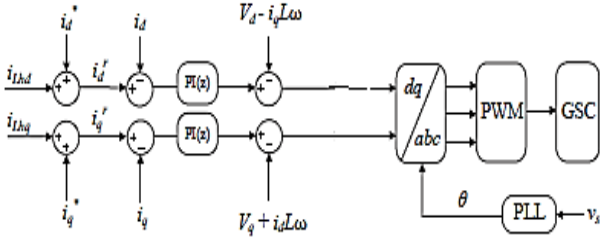


Fig. 4. Proposed schema of the control of the shunt active filter in the GSC.

#### D) Controller design of RSC and GSC

A proportional-integral PI controller on both side converters (RSC and GSC) is used to retain the magnitude of the target signal at a constant value equal to that of the reference value. The configuration of the controller depends on the internal parameters of the machine for the rotor-side converter, and the implementation of the regulator is detailed in [19]. For the GSC there are two loops: the dc bus voltage and the grid side converter reactive power which is the outer loop whereas the inner loop is for current control.

- Outer control loop of the dc voltage

The dc bus voltage is modelled as follow :

$$C_{dc} p V_{dc}^2 = -\frac{3}{2} V_{qf} I_{qf} = \delta_{dc} \quad (9)$$

$$C_{dc} p V_{dc}^2 = \delta_{dc} = (K_{pdc} + \frac{K_{i dc}}{p})(V_{dc}^{*2} - V_{dc}^2) \quad (10)$$

$$\frac{V_{dc}^2}{V_{dc}^{*2}} = \frac{\frac{1}{C_{dc}}}{p^2 + \frac{K_{pdc}}{C_{dc}}p + \frac{K_{i dc}}{C_{dc}}} (p K_{pdc} + K_{i dc}) \quad (11)$$

Where  $\delta_{dc}$  is the output of the q axis dc bus voltage controller  $K_{pdc}, K_{i dc}$  are proportional and integral gains respectively,  $V_{dc}^*$  is the reference dc bus voltage. The PI control parameters are calculated by comparing the denominator of the transfer function obtained in (11) to the Butterworth polynomial. That is :

$$p^2 + \frac{K_{pdc}}{C_{dc}} + \frac{K_{i dc}}{C_{dc}} = p^2 + \omega_{0dc} p \sqrt{2} + \omega_{0dc}^2 \quad (12)$$

$$\begin{cases} K_{pdc} = C_{dc} \omega_{0dc} \sqrt{2} \\ K_{i dc} = C_{dc} \omega_{0dc}^2 \end{cases} \quad (13)$$

- Inner control loop of currents

The implementation of the current controller is shown in Fig. 3. The reference "q" and "d" axis GSC voltages can be expressed as :

$$\begin{cases} V_{df} = \delta_{df} - \omega_s L_f I_q \\ V_{qf} = \omega_s L_f \sigma I_d + V_q + \delta_{qf} \end{cases} \quad (14)$$

Where the controller outputs are defined as :

$$\delta_{qf} = R_f I_q + L_f p I_q = (K_{pq} + \frac{K_{iq}}{p})(I_q^{*2} - I_q^2) \quad (15)$$

$$\delta_{df} = R_f I_d + V_d + L_f p I_d = (K_{pd} + \frac{K_{id}}{p})(I_d^{*2} - I_d^2) \quad (16)$$

$$\frac{I_q^2}{I_q^{*2}} = \frac{\frac{1}{L_f}}{p^2 + \frac{R_f + K_{pq}}{L_f} p + \frac{K_{iq}}{L_f}} (p K_{pq} + K_{iq}) \quad (17)$$

The current controller parameters are calculated by the following expression :

$$p^2 + \frac{R_f + K_{pq}}{L_f} p + \frac{K_{iq}}{L_f} = p^2 + \omega_{0q} p \sqrt{2} + \omega_{0q}^2 \quad (18)$$

The gains of the current regulator are expressed by

$$\begin{cases} K_{pdc} = -R_f + L_f \omega_{0qf} \sqrt{2} \\ K_{i dc} = L_{dc} \omega_{0qf}^2 \end{cases} \quad (19)$$

The converters switching frequency  $f_{sw}$  chosen is 4 kHz. Given that the switching frequency, is 4 kHz, thus the bandwidth frequencies of the inner loop and outer loop are given by the following expressions :

$$\omega_{0qf} = \omega_{sw} / 10 \quad (20)$$

$$\omega_{0dc} = \omega_{0qf} / 10 \quad (21)$$

### III. HARMONIC CURRENT IDENTIFIER

This section explains how the harmonic detection technique SRF is implemented, as previously discussed.

$$\begin{bmatrix} i_d \\ i_q \end{bmatrix} = \sqrt{\frac{2}{3}} \begin{bmatrix} \cos(\theta) & \cos(\theta - \frac{2\pi}{3}) & \cos(\theta - \frac{4\pi}{3}) \\ -\sin(\theta) & -\sin(\theta - \frac{2\pi}{3}) & -\sin(\theta - \frac{4\pi}{3}) \end{bmatrix} \begin{bmatrix} i_a \\ i_b \\ i_c \end{bmatrix} \quad (22)$$

As the same in the theory of the instantaneous reactive power, here there is d and q contain a DC components and a multiple of AC components, such as :

$$\begin{aligned} i_d &= \bar{i}_d + \check{i}_d \\ i_q &= \bar{i}_q + \check{i}_q \end{aligned} \quad (23)$$

The harmonic currents references obtained by:

$$\begin{bmatrix} i_{dref} \\ i_{bref} \\ i_{cref} \end{bmatrix} = \begin{bmatrix} \cos(\theta) & \sin(\theta) \\ \cos(\theta - \frac{2\pi}{3}) & \sin(\theta - \frac{2\pi}{3}) \\ \cos(\theta - \frac{4\pi}{3}) & \sin(\theta - \frac{4\pi}{3}) \end{bmatrix} \begin{bmatrix} \check{i}_{dref} \\ \check{i}_{qref} \end{bmatrix} \quad (24)$$

#### IV. RESULTS AND DISCUSSION

The system shown in Fig. 1 was modeled and simulated in the Matlab/Simulink associated with SimPowerSystem toolbox to analyze the control strategy proposed by DFIG/APF system. The parameters of DFIG, DC link filter, and nonlinear load used in this study are presented in Tables : 1; 2; and 3 respectively.

**Table 1.** Doubly fed induction generator parameters.

Magnitudes and parameters	Value with unit
Rated power	$P_s = 1.5 \text{ Mw}$
Source voltage	$V_s = 690\text{V}$
frequency	$f_s = 50\text{Hz}$
Stator resistance	$R_s = 2.6 \text{ m}\Omega$
Rotor resistance	$R_r = 2.9 \text{ m}\Omega$
stator inductance	$L_s = 2.56 \text{ mH}$
rotor inductance	$L_r = 2.56 \text{ mH}$
Mutualinductance	$L_m = 2.5\text{e-}3 \text{ mH}$
Number of poles	$p = 2$
Switching frequency	$f_{sw} = 4 \text{ kHz}$

**Table 2.** DC link filter and capacitor parameters.

Magnitudes and parameters	Value with unit
Filter Inductance	$400 \mu\text{H}$
Filter Resistance	$19 \text{ m}\Omega$
Power grid inductance	$0.01 \text{ mH}$
Power grid capacity	$80 \text{ mF}$

**Table 3.** Non linear load.

Magnitudes and parameters	Value with unit
Input inductance	$0.56 \text{ mH}$
Input resistance R	$10 \Omega$
Load resistance	$8 \Omega$

Two cases have been investigated of device operation. In the first scenario, the generator provides the active power without the active filtering to the nonlinear load. In the second scenario, the generator provides active control and filters grid current with the same non-linear load.

##### A) Case 1

The DFIG provides active power to the electric system. The components  $i_{dr}$  and  $i_{qr}$  follow their references  $i_{dr}^*$  and  $i_{qr}^*$  respectively as shown in fig. 5 and fig 6, controlling the active and reactive powers

Fig. 7 and Fig.8. The DC link voltage remains stable and it follows its reference value which is about 1200 V (Fig. 9).

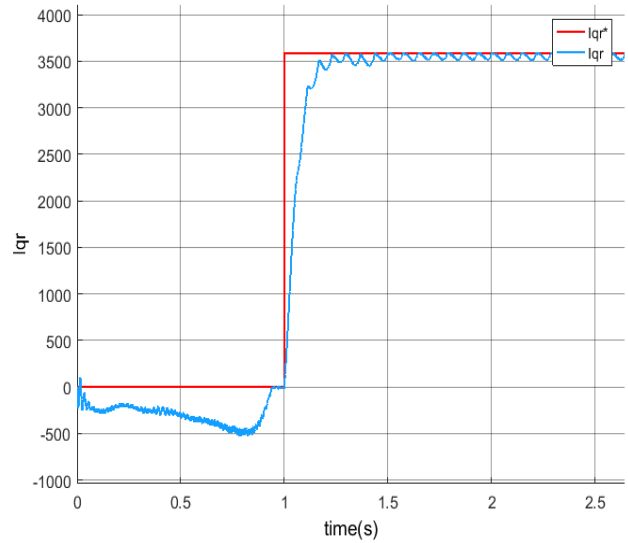


**Fig. 5.** Response of control loop of the rotor current controller  $i_{qr}$ .

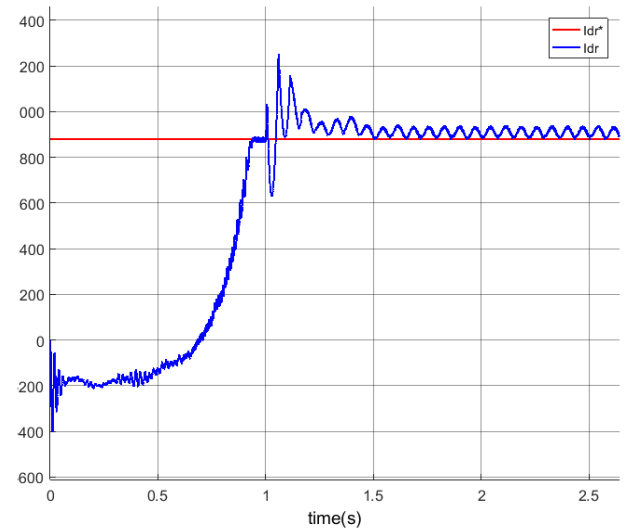


**Fig. 6.** Response of control loop of the rotor current controller  $i_{dr}$ .

The waveforms of the electric grid currents are obtained for the system running in generator mode feeding a nonlinear load for the generator speed of 149.75 rad/s (Fig. 10). To evaluate the harmonic content of current, the total harmonic distortion (THD) is the ratio between the root mean square value of the entire harmonic content and the root mean square (r.m.s) value of the fundamental frequency, and it's given in the expression :

$$\text{THD}_i = \sqrt{\sum_{h=2}^{\infty} \left(\frac{I_h}{I_1}\right)^2} \quad (25)$$

With :  $I_1$  the rms value of the fundamental current and  $I_h$  the rms values of the different harmonics of the current.

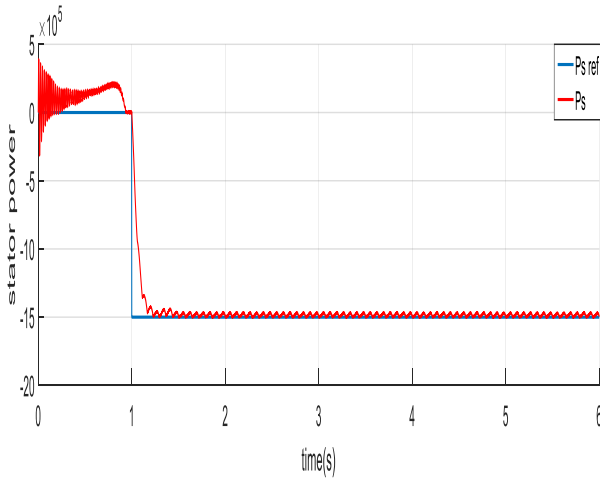


Fig. 7. Response of active ( $P_s$ ) power delivered to the electric grid.

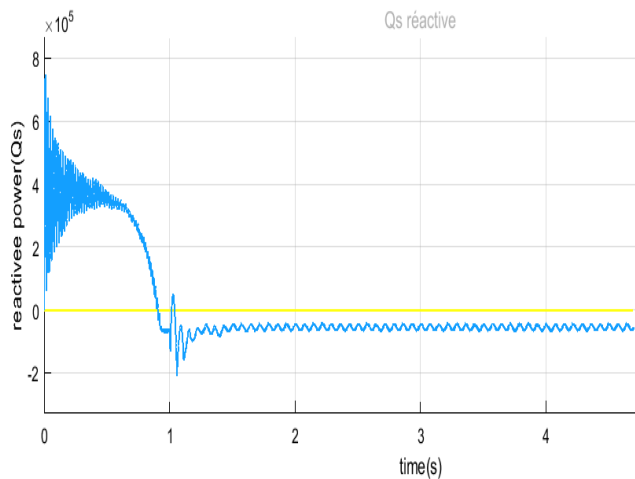


Fig. 8. Response reactive ( $Q_s$ ) power delivered to the electric grid.

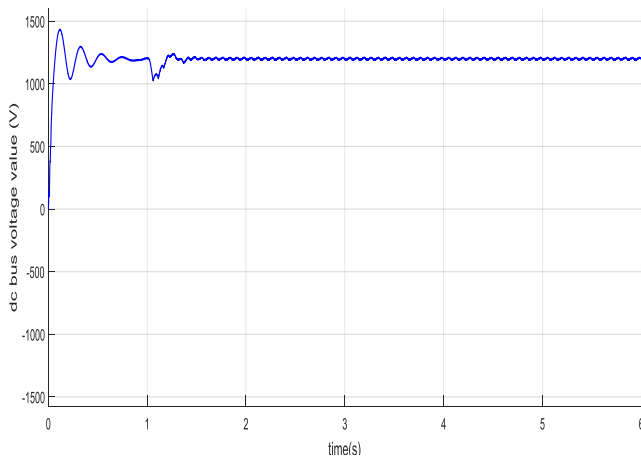


Fig. 9. Response of control loop of the dc link voltage.

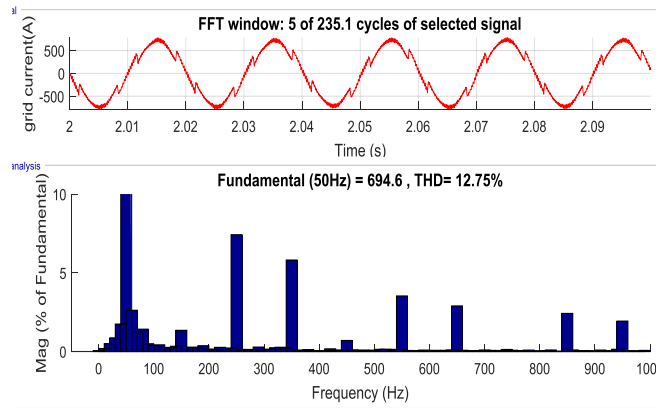


Fig. 10. The waveform current of grid.

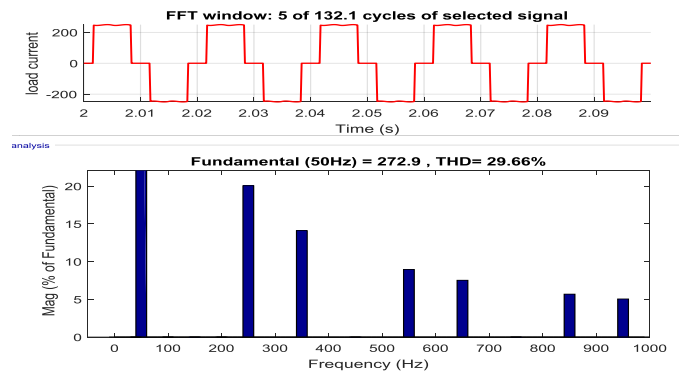


Fig. 11. Spectrum of the load current.

The current waveform at the point of common coupling PCC is distorted and shows THD of 12.75% at 149.75 rad/s, in Fig. 10. The current spectrum of the electric grid shows that among the main harmonics that contribute to this distortion are the order harmonics (5th. and 7th.). The load currents are distorted and show a total harmonic distortion (THD) equal to 29.69% in fig.11.

**B) Case 2**

The active filtering function was added to the GSC control loop of the wind system based DFIG. For this, the synchronous reference frame was applied to calculate the harmonic current content of the nonlinear load, which was added as reference to the current control loop of the GSC. The results of the power control are the same in both cases due to the similar control algorithm applied to RSC (Fig.7, Fig.8).

Fig. 12 illustrates the waveforms of the electric grid currents, obtained from the system running with active filtering function, feeding a non-linear load. It's obvious that the THD of the electric grid current was decreased. Previously the electric grid current had a THD of 12.75 %. Due to the active filtering

function added to the grid side converter of electric grid, the THD was reduced to 1.98 %.

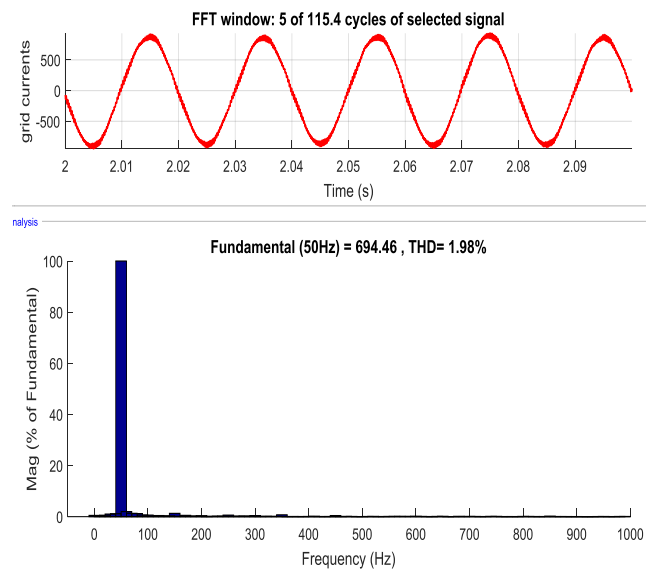


Fig. 12. Waveform of grid current after performing the filtering in the grid side converter.

## V. CONCLUSION

This study analyzed and tested the integration of filtration functions in the GSC of double-fed induction generator using Matlab Simulink environment. A vector control technique was applied to control of back to back converter where flux vector control was applied on the rotor side converter RSC whereas voltage oriented control was induced for the control of grid side converter GSC. Vector control strategy is used since it is one of the most often extended control techniques for converter control. It is characterized by easy deployment and offers strong performance features. The gain design of the PI controllers of the inner loop and outer loop of the GSC was exposed in detail. This proposed DFIG based WECS with an integrated active filter has proven its capability in terms of compensation of the harmonic in the ac power supply. The THD of the electric grid current was reduced from 12.75 % to 1.98 % which reflects the efficiency of the proposed filtering method and the improved power quality in the grid.

## VI. REFERENCES

- [1] A. El Kachani, El Mahjoub Chakir, A. A Laachir, A Niaaniaa, J. Zerouaoui, T. Jarou, *DFIG-Based Wind Turbine With Shunt Active Power Filter Controlled By*

- Double NonLinear Predictive Controller*, World Academy of Science Engineering And Technology, International Journal of Energy and Power Engineering, Vol. 9, no 12, pp. 1515-1522, 2017.
- [2] D. Kairus, R. Wamkeue, B. Belmadani, M. Benghanem, *Variable structure control of DFIG for wind power generation and harmonic current mitigation*, Advances in Electrical and Computer Engineering, Vol. 10, no 4, pp. 167-174, 2010.
- [3] H. Benbouhenni, Z. Boudjema, A. Belaidi, *A Direct Power Control of the Doubly Fed Induction Generator Based on the Three-Level NSVPWM Technique*, International Journal of smarts Vol.3, No.4, December 2019.
- [4] Adolfo R. López-Núñez, Jesús D. Mina, Gabriel Calderón Oscar Hernández, Jesús Aguayo, Jesus E. Valdez-Resendiz, *Voltage harmonics mitigation in a wind energy conversion system through the pq theory implementation in a three port back to back converter*, International Transactions on Electrical Energy Systems, Vol. 30, no 1, pp. e12180, 2020.
- [5] S. M. Zahim. I. Erlich, *Control of DFIG based Wind Turbine Converter using Continuous and Discontinuous PWM: A Comparative Study*, IFAC Proceedings Volumes, vol. 45, no 21, pp. 542-547, 2012.
- [6] H. Djeghloud, A. Bentounsi, H. Benalla, *Simulation of a DFIG-Based Wind Turbine with Active Filtering function using Matlab/Simulink*, The XIX International Conference on Electrical Machines-ICEM 2010. IEEE. pp. 1-7, 2010.
- [7] S. Rahmani, A. Hamadi et K. A-Haddad, *A comprehensive analysis of hybrid active power filter for power quality enhancement*, in IECON 2012 - 38th Annual Conference on IEEE Industrial, Electronics Society, pp. 6258–6267, October 2012.
- [8] A. Touati, R. Majdoul and M. L. Pierre, *Harmonic mitigation using shunt active filtering function based a wind energy Conversion System equipped with double fed induction generator DFIG*, IEEE, 4th International Conference on Electrical and Information Technologies ICEIT. pp. 1-6, 2020.
- [9] R. M. Sumanth et M. Purushotham, *Active Filtering Capability for WECS with Doubly Fed Induction Generator by using GSC*, 2016.
- [10] R. R. Souzaa, A. B. Moreirab, Tarcio A. S. Barros, E. Ruppert, *A proposal for a wind system equipped with a doubly fed induction generator using the Conservative Power Theory for active filtering of harmonics currents*, Electric Power Systems Research Vol. 164 , pp.167–177, 2018.
- [11] A. B. Moreira a, b, Tarcio A. S. Barros b, Vanessa S. C. Teixeira, Ernesto Ruppert, *Power control for wind power generation and current harmonic filtering with doubly fed induction generator*, Renewable Energy .Vol. 107, pp. 181-193, 2017.
- [12] M. Boutoubat, L. Mokrani, M. Machmoum, *Control of a wind energy conversion system equipped by a DFIG for active power generation and power quality improvement*, Renew. Renewable Energy, 2013, Vol. 50, pp.378-386, 2013.

- [13] V. S. R. V Oruganti., A. S Bubshait., , V. S. S. S. S , Dhanikonda., M. G, Simões, *Real-time control of hybrid active power filter using conservative power theory in industrial power system*, IET Power Electron. Vol. 10, no 2, pp. 196-207, 2017.
- [14] B. Singh, J. Solanki, *A Comparison of control algorithms for DSTATCOM*, IEEE,Trans. Ind. Electron. 56 (7) 2738e2745, Jul. 2009.
- [15] M. Kesraoui, A. Chaib, A. Meziane, A. Boulezaz, *Using a DFIG based wind turbine for grid current harmonics filtering*, Energy Convers, Manage, 968–975, 2014.
- [16] Dao Zhou, Yipeng Song and Frede Blaabjerg, *Control of Wind Turbine System*, Control of Power Electronic Converters and Systems, pp. 269-298., 2018.
- [17] L. Xu, *Coordinated control of DFIG's rotor and grid side converters during network unbalance*, IEEE Trans. Power Electron. Vol.3, pp. 1041–1049, May 2008.
- [18] S. Khojet El khil, *Vector Control of Doubly Fed Induction Generator (DFIG)*, Phd Thesis. Polytechnique institution of Toulouse, 2006.